Design Consideration of Two Candidate Propellers for Ice Breaking Vessel

Takao SASAJIMA*, Katsuyoshi TAKEKUMA* and Yoshio KAYO*

砕氷型船舶用プロペラの設計とその模型試験による評価について

笹島孝夫*・武隈克義*・加用芳男*

要旨: 氷海航行船舶の運航に際しては，船体が破壊した氷片の中で作動するプロペラおよびその軸系の挙動は，船舶本来の航行目的の達成，安全確保上非常に重要である．このため，氷海航行船舶用プロペラの設計には特に注意が払われてきた．

本論文では，砕氷型船舶用プロペラの設計手法についてレビューするとともに，設計に対する基本的考え方に基づいて，南極観測船「しらせ」について翼形状の異なる2つのプロペラを設計し，模型試験により，流体力学的特性および模擬氷による氷荷重試験を実施した結果について報告する．

現在，広く使用されている円弧翼型およびレンズ型(レーニン型)翼断面プロペラの流体力学的性能（単独特性およびキャビテーション性能），および氷荷重（アイスミリング荷重）が明らかとなり，翼断面形状の実用的な選定のために有用なデータを提供している．

Abstract: The propellers for ships operating in the Antarctic and Arctic regions encounter fragments of ice and sometimes are damaged according to the severity of ice load. The design of propellers for such ships is quite different from that of conventional ships, since in designing the propeller geometry, not only hydrodynamic performances requested are to be satisfied but also blades are to be strong enough to stand ice-milling load.

This study deals with the effect of the geometry of the propeller on performances in open-water and in ice. Two candidate propellers with different blade shape, ogival and lenticular sections were designed for the Japanese icebreaker SHIRASE, by employing the existing ice-milling load estimation method of JAGODKIN and the blade-propeller shaft strength calculation method of IGNATJEV.

The results show the specific features of each propeller blade section for propellers of icebreakers. Also, the existing methods for estimating the ice-load are found useful.

1. Introduction

In the course of the design of the propellers for a ship operating in ice-covered waterways in the Antarctic and Arctic regions, the following properties are to be examined as the fundamental requirements for the propeller:

(1) High propulsive performance for operation in open water,

(2) High thrust in navigation in ice-covered waterways for both ahead and astern conditions,

* 三菱重工業(株)長崎研究所. Nagasaki Technical Institute, Mitsubishi Heavy Industries, Ltd., 3-48, Bunkyo-machi, Nagasaki 852.

(3) Sufficient strength of propeller blades to avoid damage due to ice load.

For this purpose, selection of outline and blade section shape is of primary importance in designing propellers. Up to the present, two types of propellers, namely, ogival section and lenticular section have been adopted to the propellers for the existing ships operating in ice-covered waterways.

However, there has been little information on the effect of the propeller parameters on both hydrodynamic and ice-milling characteristics. Thus, investigations were made on the propeller for the Japanese icebreaker SHIRASE. Two candidate propellers were designed for the ship and were tested by model experiments, namely, propeller open water test, cavitation test and ice-milling test.

This paper outlines the design of the two candidate propellers, model experiments and analysis. The procedure of design in connection with the choice of material property is reviewed and hydrodynamic and ice-milling characteristics of both propellers are presented.

2. Design of Two Candidate Propellers

2.1. Design condition

Two candidate propellers were designed for the Japanese icebreaker SHIRASE, which will replace the old FUJI operating in Lützow-Holm Bay. The principal dimensions of the new vessel are shown in Table 1 (SASAKI *et al.*, 1980). This vessel is expected to have the capability of continuous icebreaking in level ice of 1.5 m in thickness at 3 kn.

Table 1. Principal particulars of the SHIRASE.

Hull	L_{wL}	=124.00 m
	B_{wL}	= 27.00 m
	B_{MAX}	= 28.00 m
	D	= 14.50 m
	d	= 9.25 m
	Δ	= 17 440 t
Engine	SHP	= 30 000 PS
	N	= 160 rpm
Propeller	D_{wing}	= 4.900 m
	D_{center}	= 4.900 m
	d_{shaft}	≦660.00 mm
Speed	V_{max}	≧ 19 kn
	$V_{cruising}$	≅ 15 kn

2.2. Design procedure

Design procedure of the propellers for ice-going vessels is a little different from the one for conventional propellers, since the propellers not only have to produce sufficient thrust to overcome the ice resistance in the continuous icebreaking operation but also have to stand the various kinds of ice load to blades.

IGNATJEV, based on the survey of the propeller troubles of ice-going vessels, developed the design procedure of blade section considering ice load (IGNATJEV, 1964). He also developed the design chart for the propellers with lenticular blade sections (IGNATJEV, 1966), which are considered to be favorable in regard to ice-milling load.

Since the lenticular blade section was applied to the propellers for Russian nuclear-powered icebreaker LENIN, it is sometimes called Lenin-type.

Ogival blade sections have also been widely used because of their symmetry to the mid-chord point since the backing characteristics are also important. The propellers for the FUJI belong to this type, and that is why two kinds of blade section, lenticular and ogival, are compared in this study.

Figure 1 summarizes the design procedure of propellers for ice-going vessels. The design calculation was conducted for the wing propellers since interaction with ice was considered to occur more frequently for the wing propellers than for the center propeller. The procedure and the data used particularly in this design are summarized in the following (EDWARDS, 1976):

(1) Propeller diameter is chosen considering the arrangement, empirical formulas (IGNATJEV, 1966; MELBERG *et al.*, 1970; MATHEWS, 1975) and existing vessels.

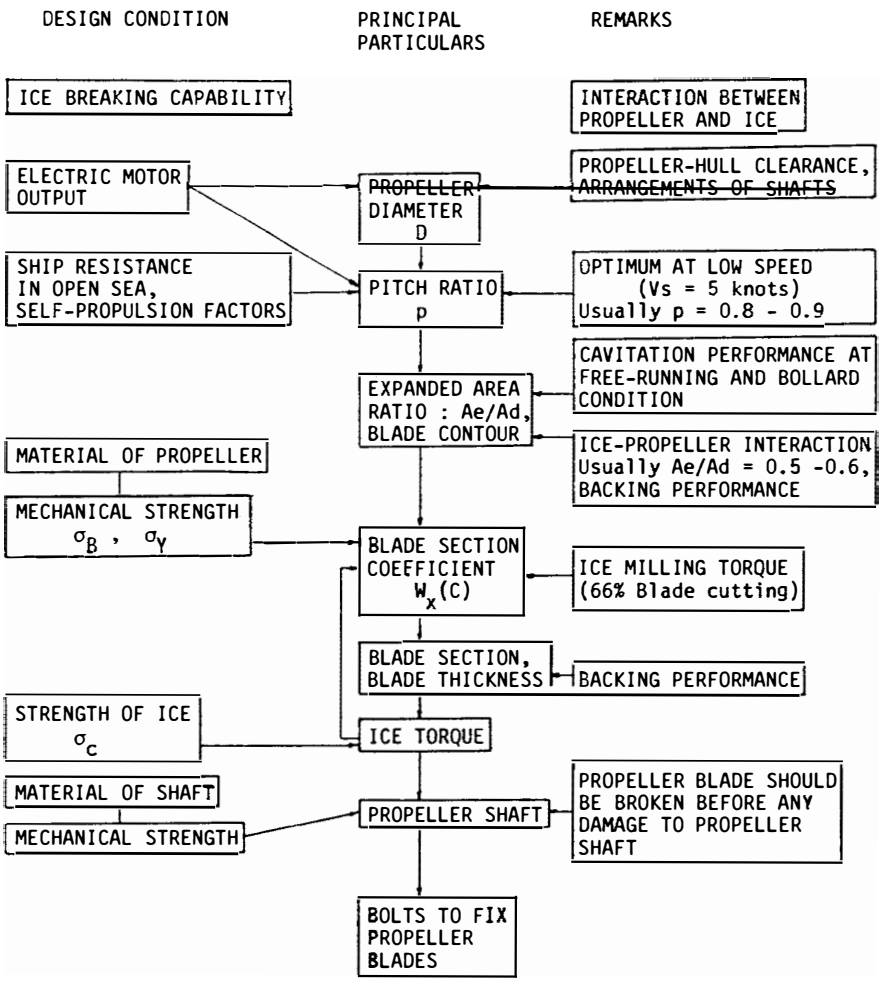

Fig. 1. Flow chart of propeller design procedure for ice-going vessels.

(2) Lenin-type blade contour was chosen for the propeller with lenticular blade section according to IGNATJEV (1964), while blade contour for the propeller with ogival blade section was made similar to those of the old FUJI and the recent Russian icebreaker ERMAK.

(3) The pitch ratio was determined to give sufficient thrust in the continuous icebreaking condition, *i.e.* at $V_s=3$ kn. Expanded area ratio was chosen with reference to cavitation criteria for the free running condition at the maximum motor output and for the continuous icebreaking condition. In determining both parameters, data of existing icebreakers were also taken into consideration. In estimating the ship speed in the free running condition and the thrust in the bollard and continuous icebreaking conditions, the Wageningen B-series (LAMMEREN *et al.*, 1969) and Ignatjev's propeller chart (IGNATJEV, 1966) were used for ogival and lenticular propellers, respectively.

(4) Resistance for the continuous icebreaking condition was estimated to be about 300 t by Kasteljan's formula (KASTELJAN *et al.*, 1973).

(5) Blade strength design was done assuming the ice-milling depth of two-thirds of the blade length. Ice-milling torque was calculated by using Jagodkin's formula (JAGODKIN, 1963) and is shown in Fig. 2. The maximum estimated ice-milling torque was about 125 t·m for the ice in Lützow-Holm Bay. Also the strength of the ice was assumed as follows, referring to the published data (SASAKI *et al.*, 1978):

Crushing strength $\sigma_c=2.55$ MPa (26 kg/cm^2)
Shearing strength $\tau=0.64$ MPa (6.5 kg/cm^2)

(6) Special 13Cr stainless steel (trade name MSS, TANIGUCHI *et al.*, 1968) was chosen, based on the several years experience of its use as the propeller material of the FUJI. Mechanical properties are as follows:

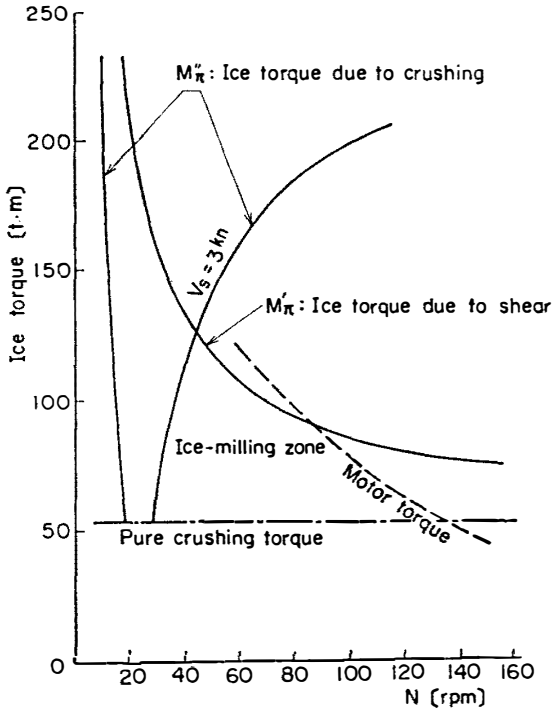

Fg. 2. Ice-milling torque estimated by Jagodkin's formula.

Tensile strength: $\sigma_t = 834$ MPA (8 500 kg/cm^2)
0.2% proof stress: $\sigma_y = 540$ MPa (5 500 kg/cm^2)
Elongation: $\xi = 0.15$

(7) Since the maximum blade stress due to ice-milling occurs at the maximum thickness point of the back side (C point, see Fig. 3) of the blade section, section modulus $W_x(C)$ was calculated at the 0.4R by using 0.2% proof stress of the material, based on the Ignatjev's method.

$$W_x(C) = 4\,993 \text{ cm}^3$$

(8) Section modulus thus obtained was non-dimensionalized and expressed as blade section coefficient k_x, the definition of which is as follows:

$$k_x = W_x/(ct^2)$$

The blade section coefficient at point C at 0.4R was analyzed to be 0.0872 for ogival and 0.0812 for lenticular blade section respectively.

(9) Two factors are important to design propeller shafts, namely the restriction of the diameter from manufacturing facility and avoidance of any damage to propeller shaft. Thus the propeller shaft was designed not to suffer any plastic deformation by the ice torque before the fracture of the blade at the face side. The steel alloy was chosen for the shaft, the mechanical strength of which is as follows:

$$\sigma_y = 451 \text{ MPa } (4\,600 \text{ kg/cm}^2).$$

The diameter of the shaft is 66 cm. Relative strength of the blade and shaft or ice torque is shown in Fig. 3.

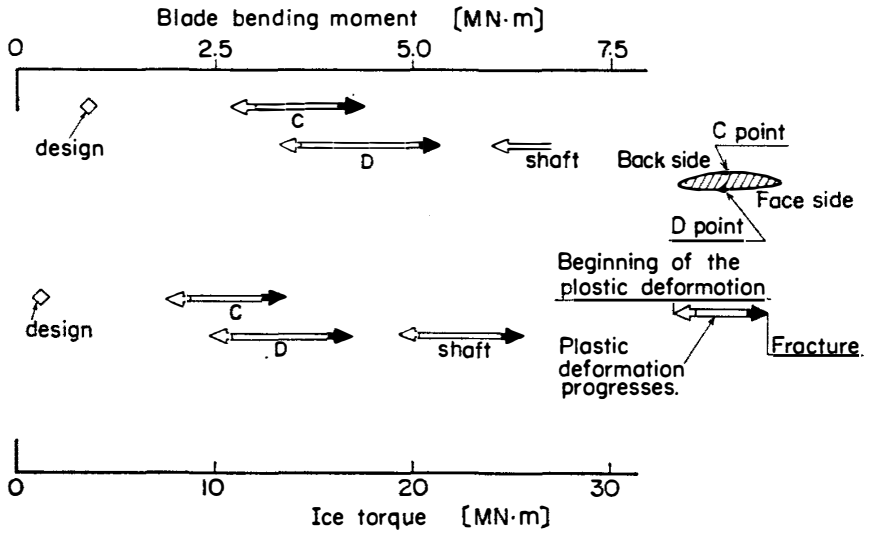

Fig. 3. Relative strength design of blade and propeller shaft.

2. 3. Results of the propeller design

The principal particulars of propellers thus designed for wing propellers are shown in Table 2. Figure 4 shows the geometry of the two candidate propellers, by photographs of their model and typical blade sections.

Table 2. Principal particulars of candidate propellers.

	Propeller A	Propeller B
D (D_{model})	4.900 m (250.000 mm)	
Ae/Ad	0.5500	
p (const.)	0.8586	0.8694
d/D	0.3061	
$t/c)_{0.7}$	0.05940	0.06126
t/R)0.4	0.0816	0.0784
$t/R)_{1.0}$	0.0163	
$k_x)_{0.4}$(D)	0.1070	0.0874
$k_x)_{0.4}$(C)	0.0872	0.0812
z	4	
Section	Mod. Ogival	Lenticular

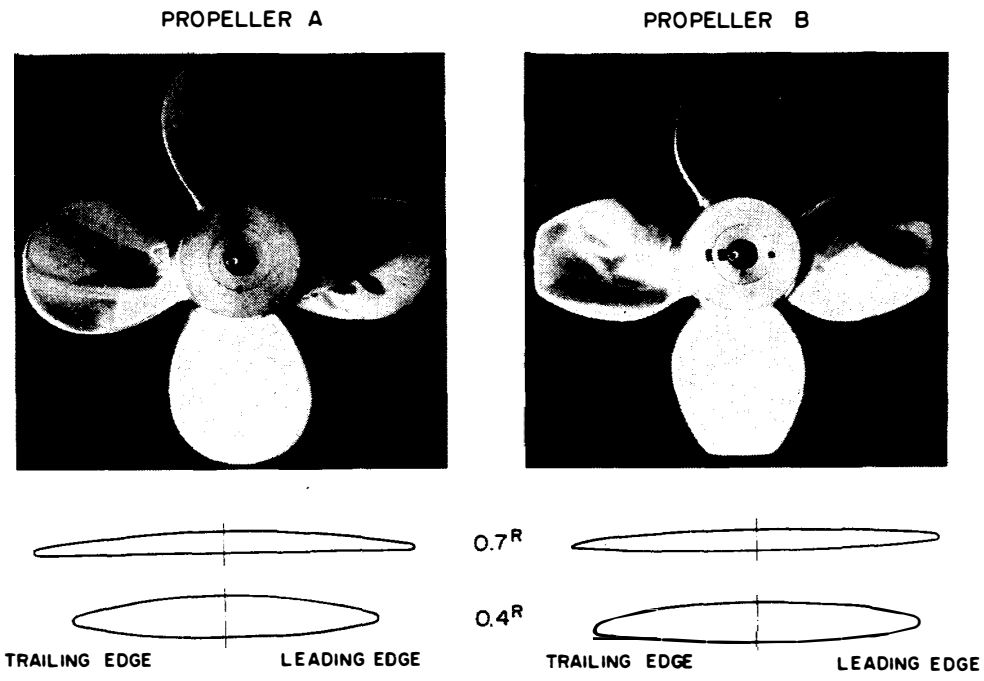

Fig. 4. Geometry of two candidate propellers.

3. Model Propellers

To study the characteristics of the two types thus designed for wing propellers of the SHIRASE, model tests were planned. In manufacturing model propellers special care was taken in order to conduct not only hydrodynamic tests but also ice-milling test.

The size of the model propellers was chosen to be 250.00 mm in diameter to avoid the unfavorable wall effect of the tunnel for cavitation test. Model propellers were cut out from the high tensile aluminum alloy bar, to get the blade strong enough to withstand the ice load in the ice-milling tests.

4. Hydrodynamic Characteristics of the Candidate Propellers

Open-water characteristics and cavitation performance were investigated first at the Nagasaki Experimental Tank, by the propeller open-water tests in the towing tank and cavitation tests in the 50×50 cm square test section cavitation tunnel.

4.1. Open-water characteristics

Figure 5 shows the comparison of the open-water characteristics, where non-dimensionalized thrust (K_T) and torque (K_Q), with propeller efficiency (e_p) are shown against advance coefficient (J).

$$K_T = T/\rho n^2 D^4$$
$$K_Q = Q/\rho n^2 D^5$$
$$e_p = JK_T/2\pi K_Q$$
$$J = v/nD$$

Propeller B shows a little better propeller efficiency than that of propeller A. Using these data, power calculation was done to see the effect of blade section on ship performances, such as ship speed at maximum motor output (30 000 PS), power for cruising speed (15 kn) and bollard thrust. The results are given in Table 3 which

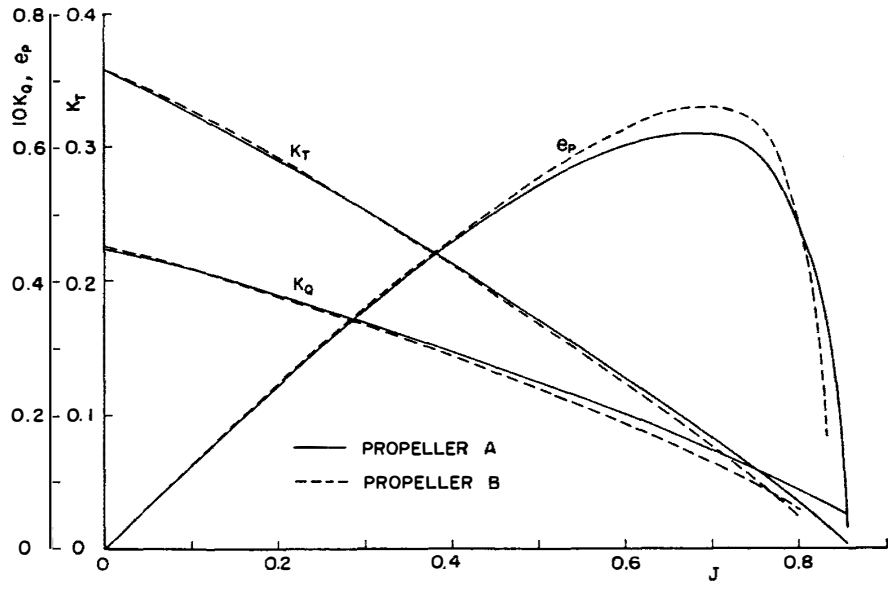

Fg. 5. Comparison of open-water characteristics.

Table 3. Hydrodynamic performance of candi d te prope l ers.

	Propeller A	Propeller B
Ship speed at maximum motor output (30 000 PS)	19. 5 kn	19. 7 kn
Power at cruising speed (15 kn)	7 420 PS	7 030 PS
Bollard thrust (123 rpm)	90. 5 t/shaft	90. 8 t/shaft

shows that propeller B has better performance in open sea conditions, while the bollard thrust is almost the same for the both propellers.

4.2. Effect of cavitation on propeller performance

To see the effect of cavitation on propeller characteristics in a very high propeller load condition, such as the continuous icebreaking condition*, thrust and torque measurements at the lowest advance coefficient obtained in the cavitation tunnel, *i.e.* $J=0.225$, were conducted by changing cavitation number σ_n, the definition of which is as follows:

$$\sigma_n=\frac{p_0+\gamma I-e}{(1/2)\rho(nD)^2}$$

where, p_0: atmospheric pressure
γ: specific weight of sea water
I: propeller immersion
e: vapor pressure
ρ: density of sea water

The results are shown in Fig. 6. It can be said from this figure that the difference in thrust breakdown characteristics of both propellers is small.

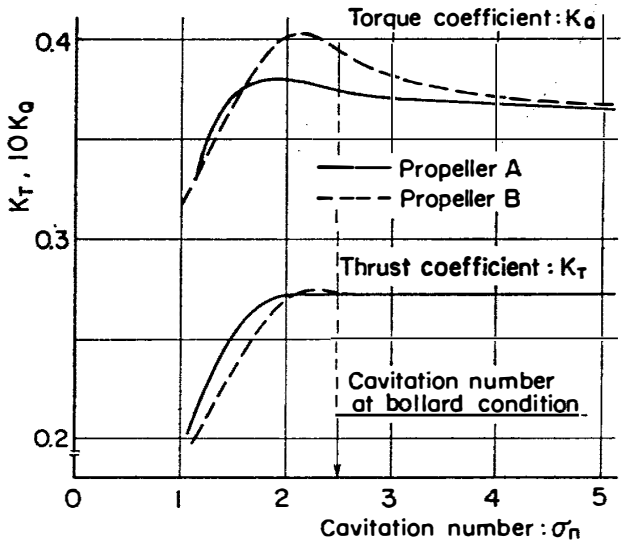

Fig. 6. Change of thrust and torque with cavitation number in bollard condition.

4.3. Effect of unsteady cavitation

The two types were designed for the wing propellers of the Japanese icebreaker SHIRASE, as mentioned before. Since the ship has to voyage from Japan to the Antarctic region before operating in ice-covered sea region, due attention should be paid also to cavitation erosion problem.

* In this study, only wing propellers were designed to manufacture the model propellers. So the characteristics of the wing propeller were applied to the center propeller in calculating speed and power without correction for pitch ratio.

Since the wake distribution in the plane of the center propeller is severer than that of the wing propellers, cavitation tests in non-uniform flow were conducted in the wake simulated for the center propeller. Figure 7 shows the simulated wake distribution used in these tests. Test conditions for the both types were calculated using the ship performance data as shown in Table 4.

Photographs of typical cavitation patterns in the conditions of the maximum motor output and very high propeller load (the minimum advance coefficient obtained

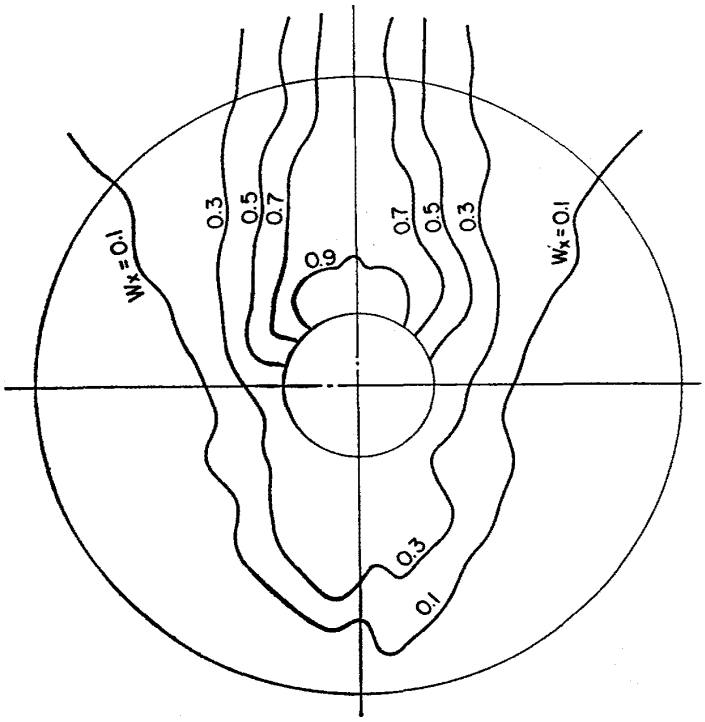

Fig. 7. Simulated wake contour curves.

Table 4. Operating condition of each propeller.

	Operating condition of propeller		Test condition	
	Propeller A	Propeller B	σ_n	K_T
Max. speed 10 000 PS/shaft	$K_T=0.123$ $\sigma_n=2.08$	$K_T=0.123$ $\sigma_n=1.980$	2.0	0.125
Cruising speed	$K_T=0.085$ $\sigma_n=4.2$	$K_T=0.084$ $\sigma_n=4.1$	4.0	0.085
Bollard cond. 10 000 PS/shaft $\eta_t=0.96$	$K_Q=0.0448$ $\sigma_n=3.15$	$K_Q=0.0452$ $\sigma_n=3.15$	3.0	0.357* (0.284)

* $K_t=0.284$ was the maximum attainable thrust coefficient in cavitation tunnel with advance speed produced by propeller only. The propeller advance coefficient in this condition was $J=0.22$.

* Estimated operation conditions of the propeller in continuous icebreaking at 3 kn are as follows: $J=0.12$, $\sigma_n=2.5$.

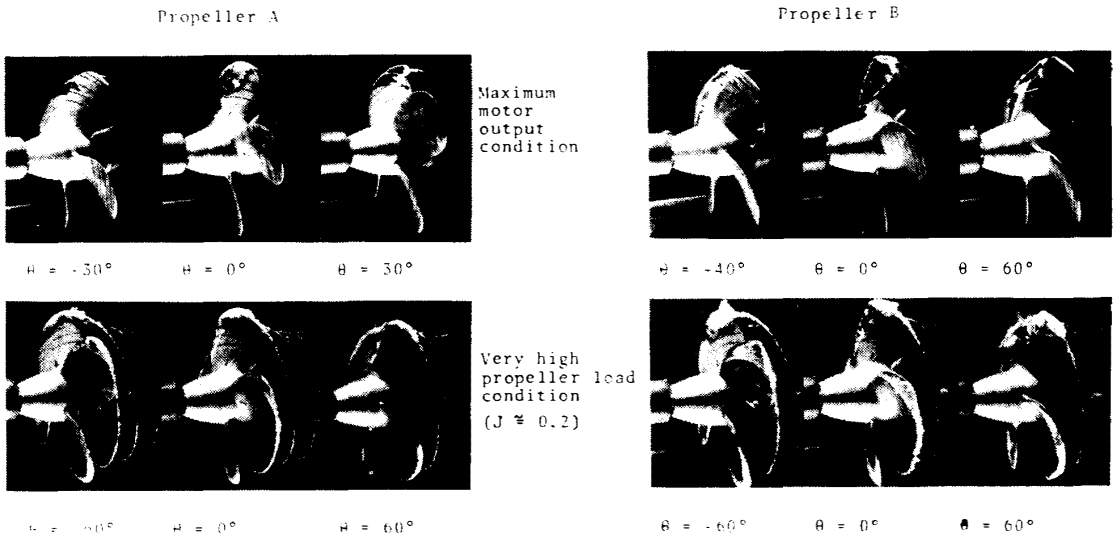

Fig. 8. Comparison of cavitation patterns in simulated wake.

in the cavitation tunnel was about 0.22*) are shown in Fig. 8. Judging from these cavitation patterns, propeller B will suffer from cavitation erosion in the maximum motor output condition due to unsteady cloud cavitation, while propeller A with ogival sections will be free from erosion. In the very high propeller load condition, such as the continuous icebreaking condition, cavitation on the blade was stable and damage will be expected in both types.

Thus the propeller with ogival blade section is preferable from the viewpoint of cavitation erosion.

5. Ice-milling Characteristics of the Candidate Propellers

5.1. Test procedure

The following measurements were conducted by using the special lathe designed for the ice-milling tests (CHARLES, 1976).

Blade bending moment (*BM*)

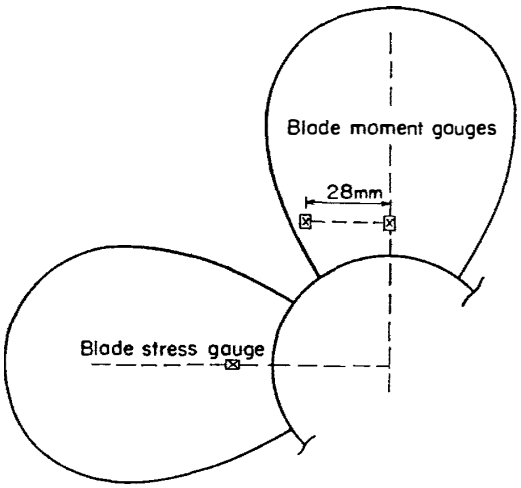

Fig. 9. Strain gauge arrangement on propeller blades

Thrust (T) and torque (Q)

Radial force (F)

Ice speed (V_s) and revolutions of propeller (n)

Figure 9 shows the strain gauge arrangement on blades, and Fig. 10 shows the arrangement of test apparatus. All the sensors were calibrated before or between the tests by putting known axial and radial forces at three points on blades.

Advance angle of the propeller blade to ice,

$$\alpha_\nu = \tan^{-1}\frac{V_s}{2\pi n R_p}$$

where V_s: advance speed of ice to propeller

R_p: center radius of milling part of the blade

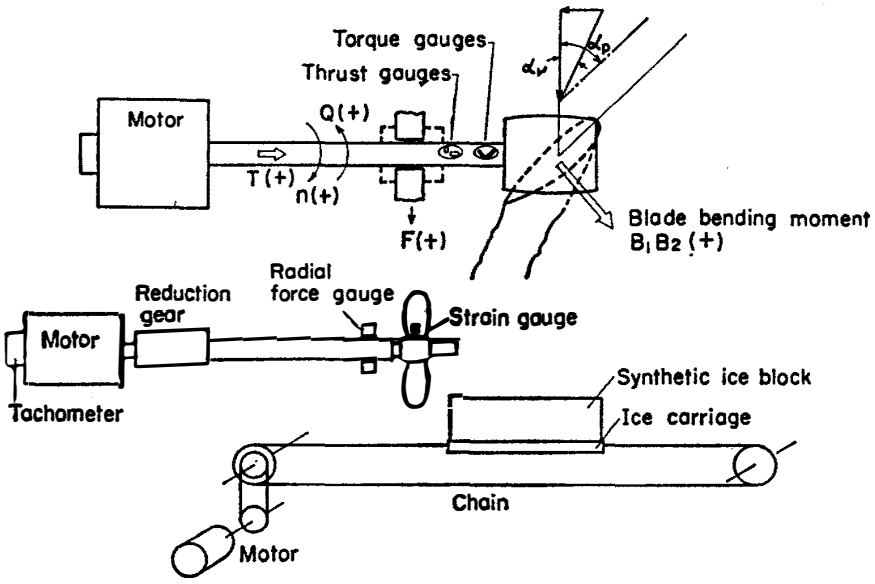

Fig. 10. Arrangement of test apparatus.

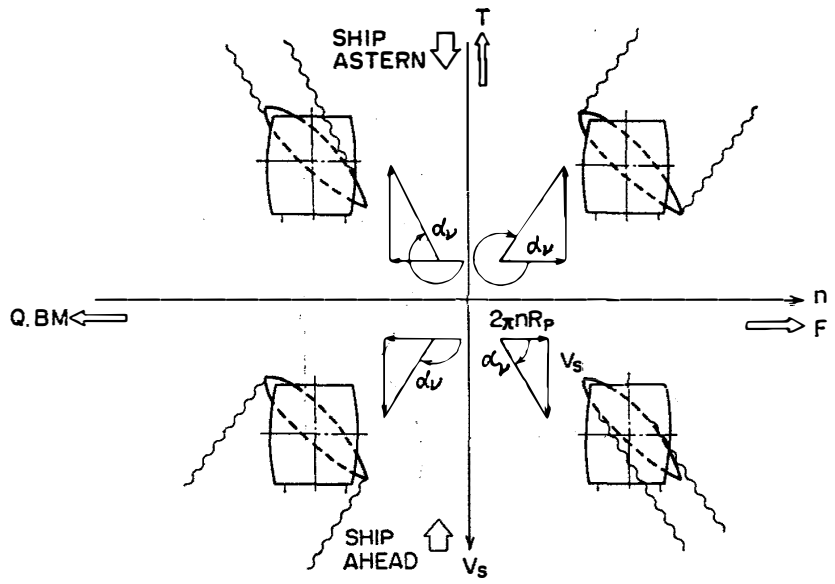

Fig. 11. Change of ice-milling condition with advance angle.

was changed from 0 to 360° by selection of the relative ice speed to the propeller and revolutions of propeller. The ice-milling condition of the propeller blades relative to the ice is illustrated in Fig. 11.

The synthetic ice, patented by the Arctec Canada, Ltd., was used in these tests, the strength of which was controlled to the model scale level. Since the scaling ratio of the model propeller λ is 19.6 in these tests, a corresponding strength of the model ice should be the following value:

$$\sigma_c)_{model} = \lambda^{-1} \cdot \sigma_c)_{ship} = 130 \text{ KPa} \quad (1.32 \text{ kg/cm}^2)$$

5.2. Test results and discussion

5.2.1. Strength of the synthetic ice

Strength of the synthetic ice was checked by uniaxial strength, flexural strength and indentation test, according to the standard procedure of Arctec Canada, Ltd. Especially the crushing strength σ_c, obtained from the uniaxial strength tests, is measured for each synthetic ice block to analyze the ice-milling data. Average values of the crushing and flexural strength of the synthetic ice are summarized in Table 5.

From these data, it can be said that, even though the data scattered considerably, the crushing strength of the synthetic ice was not so much different from the target value, *i.e.* $\sigma_c = 130$ KPa.

Indentation tests, which correspond to the ice-milling tests at advance angle of

Table 5. Mechanical strength of synthetic ice.

	Number of test pieces		Size of test pieces
Crushing strength (σ_c: KPa)	65.4±14.5 at 0.012 m/s	9	0.05×0.05×(0.13–0.17) m
	95.6±23.5 at 0.03 m/s	11	
	130.0±28.0 at 0.049 m/s	4	
Flexural strength (σ_f: KPa)	59.4±11.7	5	0.22×0.05×0.03 m

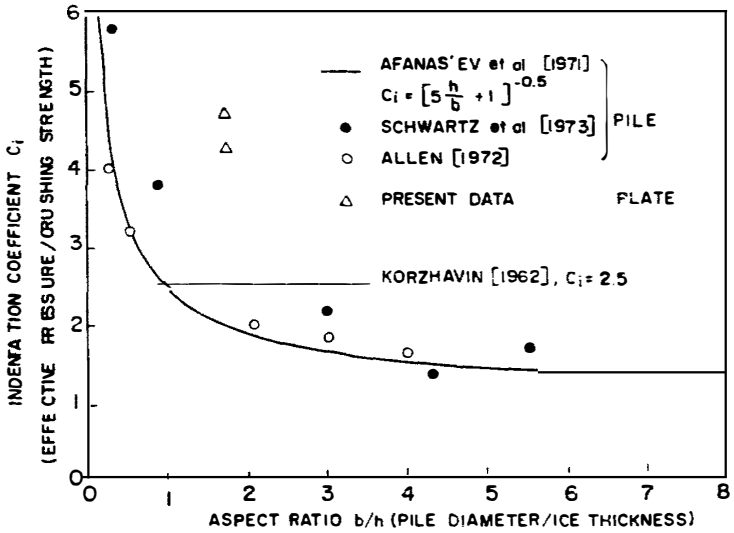

Fig. 12. Comparison of indentation test results with existing data.

90°, were conducted to check the correlation of synthetic ice data with saline ice data. The test data are compared with the existing data for piles in saline ice (CHARLES, 1976), as shown in Fig. 12.

The present test data on the flat plate are found considerably larger than the existing data. But if we take into account the difference in the shape of the test piece and in the configuration of indentation (in the case of existing data, piles are pierced through ice sheets, while in this case the lower end of the plate is within ice and working as a cantilever), the present results on the synthetic ice are considered to be correlated with those on the saline ice.

5. 2. 2. Results of ice-milling tests

All the data were recorded with the TEAC-R81 casette data recorder and replayed on the visicorder to see the blade bending moment, shaft thrust and torque, and side force due to ice-milling. Typical examples are shown in Fig. 13, and the condition of the test run A_7 and B_7 is shown in Table 6.

Figure 14 shows some photographs taken during the tests.

Of the data obtained in each ice-milling test, the maximum blade bending moment, propeller thrust and torque, were picked up from the viewpoint of engineering application. To take the relative strength of the ice into account, those quantities were divided by the crushing strength of the synthetic ice block. The results are compared

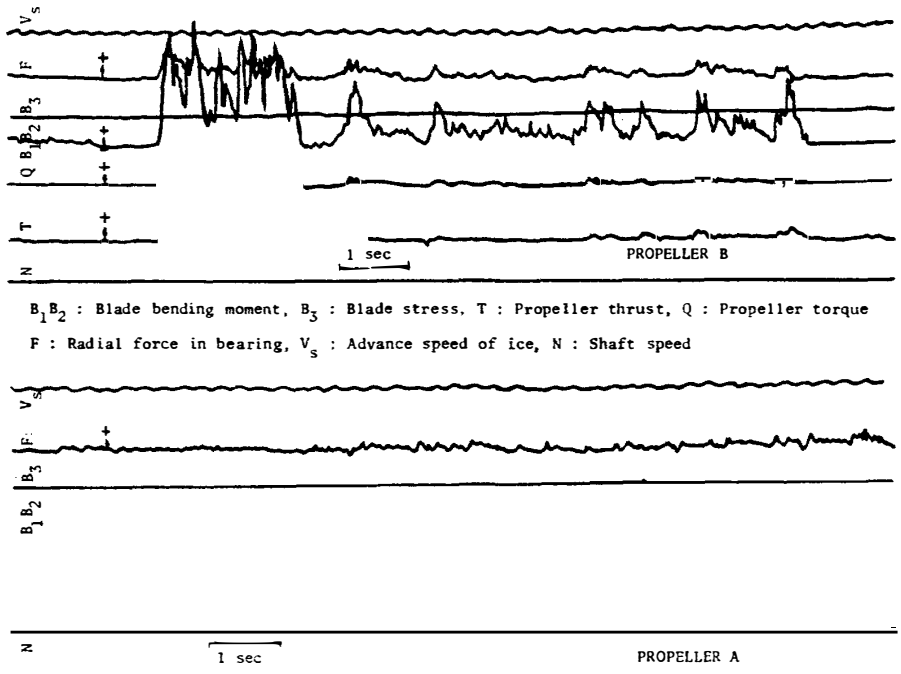

Fig. 13. Examples of visicorder records of ice-milling test results.

Table 6. Test condition for Fig. 13.

Mark	Propeller	Cutting depth (%)	n (rps)	V_s (m/s)	Blade bending
A_7	A	66	0	0	B_1B_2
B_7	B	66	0	0.036	B_1B_2

between two model propellers and shown in Figs. 15, 16 and 17, where the cutting depth of the blade and the advance speed of the ice block are chosen as parameters. Even though it is hard to draw quantitative conclusions from these data directly due to limited number of data points and scattering of them, a general tendency that propeller B suffers less load from ice can be recognized.

In an effort to see this tendency more clearly, it was tried to draw a mean line through these scattered data, especially for the case of 33% blade depth cut at the milling speed of 0.05 m/s, taking the tendency of the published data (EDWARDS, 1976) into consideration and compared between the two propellers as shown in Fig. 18.

PROPELLER A, $\alpha_v=30°$ PROPELLER B, $\alpha_v=90°$

Fig. 14. Ice-milling tests for propellers A and B.

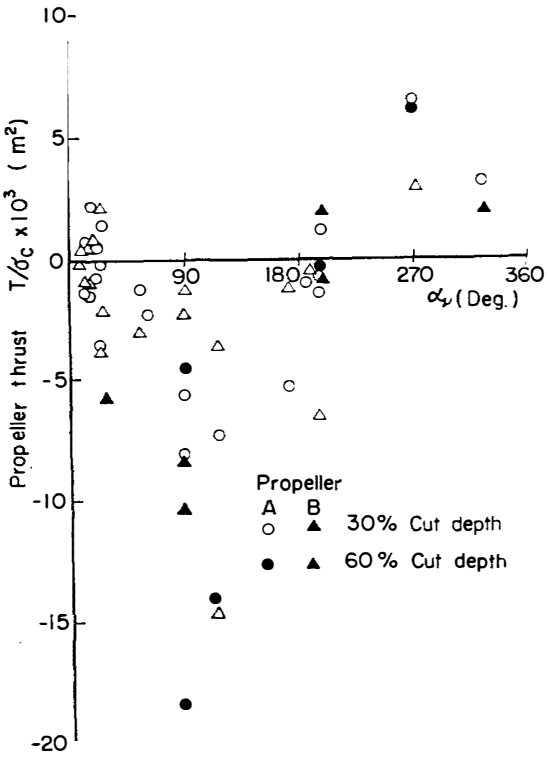

Fig. 15. Ice-milling test results (propeller thrust).

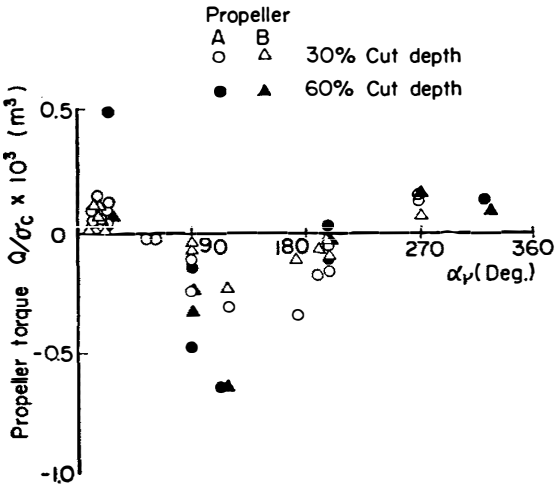

Fig. 16. Ice-milling test results (propeller torque).

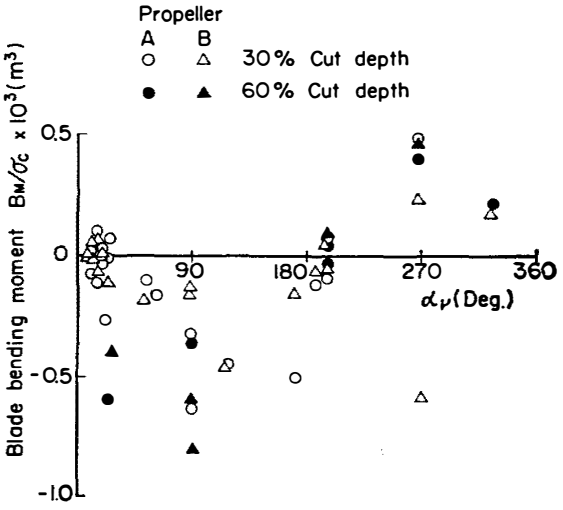

Fig. 17. Ice-milling test results (blade bending moment).

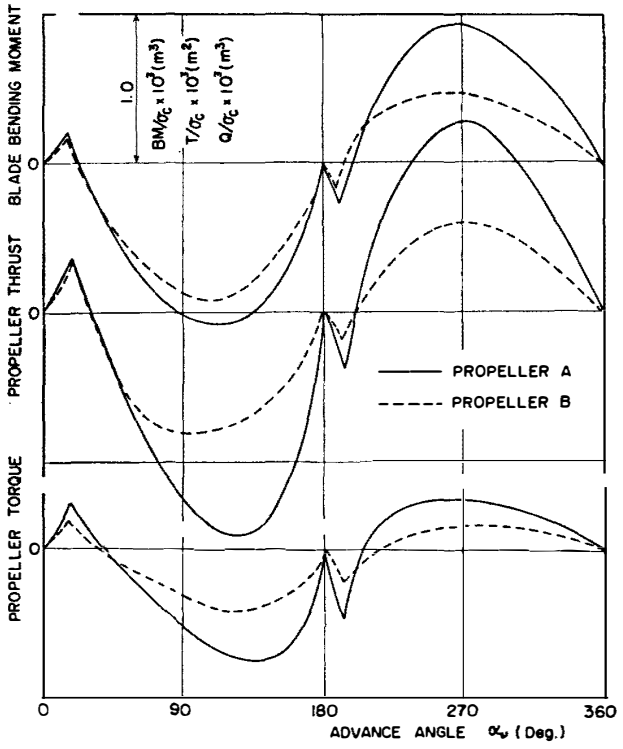

Fig. 18. Comparison of ice-milling loads beween propellers A and B.

Near the design advance angle of the propeller, *i.e.* $\alpha_v \simeq 25°$, the ice load is almost the same for both propellers, while in other conditions, especially at $\alpha_v = 90°$ and 270° where the propeller blades indent the ice without rotational speed, propeller B shows a considerably low ice load to blades and propeller shaft. Also it is pointed out that the pure crushing condition of the blade when the ship is reversing ($\alpha_v = 200°$), which happens frequently in the ramming operation, the ice load to propeller B is much smaller than that to propeller A.

Thus it can generally be said that, the propeller with the lenticular blade section, *i.e.* propeller B, is preferable from the ice load point of view.

Then the blade stress of the full scale propeller in the design condition (pure crushing condition, $\alpha_v=25°$) was estimated by the following formula using the model test data:

$$\sigma_s=\frac{M_b/\cos\beta}{W_x(C)}=\frac{[M_b/\sigma_c]_M\cdot\sigma_c)s/\cos\beta}{k_x\cdot c\cdot t)^2}$$

where M_b: blade bending moment
β: blade pitch angle at the radius of point C
σ_c: crushing strength
k_x: blade section coefficient
c: blade width
t: blade thickness

Since the blade strength design was done at 0.4 radius and in the condition of 66% blade cut, $(M_b/\sigma_c)_M$ in that condition was estimated from the data of 33% blade cut condition, assuming that the apparent ice load per unit blade length is unchanged for the case of 66% blade cut. The results are shown in Table 7. From these data it can be said that almost the same safety factor was obtained for both propellers, which means that the design procedure using Jagodkin's and Ignatjev's formula is useful.

Figure 18 also clearly shows that the fracture of blade will easily happen when the blades are forced to indent a large ice block without rotation. Such conditions should be carefully avoided by the operation of the ship.

Table 7. Check of the propeller design based on ice load by using model test data.

		Propeller A	Propeller B
Geometrical parameters at 0.4R	k_x (c)	0.0872	0.0812
	c (m)	1.434	1.530
	t (m)	0.1999	0.1921
	$\cos\beta$	0.826	0.822
Test data	M_b/σ_c	0.21×10^{-3}m³	0.185×10^{-3}m³
Full scale ice data	σ_c	2.55 MPa (260 t/m²)	
Blade stress	σ (1/3 blade cut)	131 MPa (1 332 kg/cm²)	103 MPa (1 049 kg/cm²)
	σ (1/3 blade cut)	207 MPa (2 115 kg/cm²)	200 MPa (2 042 kg/cm²)
Material strength	σ	539 MPa (5 500 kg/cm²)	
Safety factor	analyzed	2.6	2.7
	designed	3.0	

6. Concluding Remarks

Evaluation of two candidate propellers designed for the Japanese icebreaker SHIRASE, was conducted from both hydrodynamic and ice load points of view. Two

Table 8. Evaluation of candidate propellers.

Efficiency (open sea characteristics)	Propeller B
Bollard thrust	No difference
Thrust breakdown due to cavitation	No difference
Cavitation in non-uniform flow	Propeller A
Ice-milling capability	Propeller B

model propellers, namely propeller A which has the ogival section and propeller B which has the lenticular blade section, were tested in the towing tank and in the cavitation tunnel, and the special lathe was used for ice-milling tests. The results showed the comparative merits of both propellers as summarized in Table 8.

These results give some hints in selecting the geometry of propellers for ice-going vessels. In the case of the triple screw icebreaker, for example, since the wing propellers have more chances to interact with ice blocks but are relatively free from cavitation problems, propellers with lenticular blades will be preferable. On the other hand, in the case of the center propeller, since cavitation problem is severe, ogival blades will be better.

Also from these data, the well-known Jagodkin's formula for ice torque estimation and Ignatjev's formula for blade bending moment were shown to be useful in designing the propellers for icebreakers.

Acknowledgments

The authors wish to express their hearty appreciation to Mr. EDWARDS, former president of Arctec Canada, Ltd. and now president of Offshone Technology Corporation, for his guidance in conducting ice-milling tests.

The authors also thank the staff of both in the Arctec Canada, Ltd. and the Nagasaki Technical Institute, for their support to this project.

References

CHARLES, R. N. (1976): Dynamic ice forces on pier and piles, an assesment of design guidelines in the light of recent research. Report of Northwest Hydraulic Consultants Limited, Edmonton.

EDWARDS, R. Y., Jr. (1976): Methods for predicting forces encountered by propellers during interactions with ice. 3rd Lips Propeller Symposium, Drunen, The Netherlands.

IGNATJEV, M. A. (1964): Raschet prochnasti lopastei grebnykh vintov ledokolov i sudov ledobogo plavaniya (Strength calculations for propeller blade of ice-breaker and ice-going vessel). Sudostroenie, **1**, 5–7.

IGNATJEV, M. A. (1966): Grebnye Vinty Sudov Ledovogo Plavaniya (Screw Propeller for Ship Navigating in Ice). Leningrad, Sudostroenie, 114 p.

JAGODKIN, V. Ya. (1963): Analiticheskoe opredelenie momenta soprotivleniya vrashcheniya grebnogo vinta pri ego vzaimodeyslvii so l'dom (Analytic determination of resistance moment of a propeller during its interaction with ice). Probl. Arkt. Antarkt. (Probl. Arct. Antarct.), **13**, 79–88.

KASTELJAN, V. I., RYVLIN, A. Ia., FADDEF, O. V. and JAGODKIN, V. Ja. (1973): Icebreakers. CRREL Draft Transl., **418**, 263 p.

LAMMEREN, W. P. A., VAN MANEN, J. D. and OOSTERVELD, M. W. C. (1969): The wageningen B-screw series. SNAME Trans., **77**, 263–317.

MATHEWS, S. T. (1975): Aspects of propulsion power of arctic vessel considering their operating environment. Proceedings of SNAME Ice Tech. Symposium, Montreal, Al–A12.

MELBERG, L. C., LEWIS, J. W., EDWARDS, R. Y., Jr., TAYLOR, R. G. and VOLKER, R. P. (1970): The design of polar icebreakers. SNAME Spring Meeting, Washington, D.C.

SASAKI, H., YABUKI, S. and SATO M. (1978): Saihyôkan "Fuji" no hyôkai kôkô to jikukei taihyô kyôdo ni tsuite (Ice-navigation and shafting strength of icebreaker "Fuji"). Nihon Hakuyô Kikan Gakkaishi (J. Marine Eng. Soc. Jpn), **13**, 716–725.

SASAKI, H., YABUKI, S. and SATO, M. (1980): Design concept of strength for icebreaker shafting. UJNR-Marine Facilities Pannel 10th Meeting, Washington, D.C.

TANIGUCHI, K., OBA, T., UEDA, S. and NAKAJIMA, M. (1968): Kyodaisen-yô kôkyôdo shintoku-shukô puropera no kaihatsu (Development of new high strength special steel propeller for big ships). Nihon Zôsen Gakkai Ronbunshû (J. SANJ), **123**, 59–73.

(*Received August 4, 1984*)